Journal of The Acoustical Society of R.O.C.,Vol.2 No.2 pp.1-16(1994)

結構聲音輻射之混合主動與被動控制

王栢村*

*國立屏東技術學院機械工程技術系

中文摘要

本文探討一具有無限長剛體屏障簡支樑的聲音輻射之混合主動與被動控制，假設一諧振點力作用於結構爲干擾源，集中質塊爲被動控制元件，加於結構可改變結構之模態性質，壓電驅動器黏貼於結構上作爲控制源，而以壓電薄膜作爲近場結構感應器，主動控制係以最小平方前饋控制爲主，以一最小化程序計算輸入驅動器之最佳控制電壓，若將被動控制與主動控制同時作用稱爲混合控制。聲音輻射能量在頻率之響應作爲評估被動、主動和混合控制之控制效果，結果顯示主動控制在接近共振激振頻率時可達到良好控制，如能適當選用被動元件，混合控制可比主動或被動控制達到較佳之聲音輻射控制，本文証明了結合主動與被動控制在結構聲音輻射之混合控制的可行性。

關鍵語：樑；聲音輻射；控制。

Hybrid Active and Passive Control for Structural Sound Radiation

Bor-Tsuen Wang*

*Department of Mechanical Engineering National Pingtung Polytechnic Institute Pingtung, Taiwan

ABSTRACT

This paper analytically studies the hybrid active and passive control of sound radiation through a simply-supported beam mounted with an infinite rigid baffle. A harmonic point force is applied to the structure as the primary source (disturbance). A concentrated mass, a passive element, is added to the structure to restructure the modal properties. The piezoelectric actuator bonded to the structure surface is applied as the secondary source (control force), while the PVDF film is used as the near-field structural sensor. Active control is performed in conjunction with the use of LMS feedforward control algorithm. A minimization process is employed to calculate the optimal control voltage applied to the actuator. Both the passive element and active control are applied simultaneously and termed as the hybrid control. The radiated power verse excitation frequencies is plotted to evaluate the effectiveness of passive, active and hyrid control. Results show that active control can provide sufficient control for excitation near the resonance. With the proper selection of pasive element, hybrid control can achieve better sound radiation control than passive or active control alone. This work demonstrates the feasibility to combine the active control mean and passive element applied to structural sound radiation control.

Keywords: beam, sound radiation, control.

1. INTRODUCTION

Structural vibration and sound radiation control has been a great deal of interest. Either passive or active control are generally applied to suppress the structural vibration so as to reduce the structural radiated sound. Passive noise control (PNC) is usually applied by adding mass, damping treatment or stiffening the structure [1,2]; however, the effective-

ness of PNC is generally inadequate for low frequency noise control application. Due to the development of fast processible personal computer, active noise cancellation methods have been drawn much attention. Steven and Ahuja [3] gave a good overview of active noise control (ANC). It is well known that ANC can achieve significant noise reduction at low frequencies. Upon the progress of sensor and actuator technology, the use of "smart", "adaptive" or "intelligent" structures involving distributed actuators, sensors and pc-based control algorithm can effectively control the sound radiation through vibrating structures. One of the frequently used distributed actuators and sensors is piezoceramic materials. The finite length of piezoelectric patch can be bonded to the surface of the structure and applied to induce or measure structural motion. Many works have been devoted to the applications of such a distributed acturator and sensor to vibration control of large structure [4-6] and to the control of structurally radiated noise [7-9].

Previous work by the author [10] applied piezoelectric actuators and accelerometers as error sensors in conjunction with the use of the concentrated mass, i.e., a passive control element, to perform hybrid structural vibration control. Results show that hybrid control performs better vibration control than passive or active control individually. This paper generally extracts this idea of hybrid active and passive control to attenuate the structurally radiated sound. A simply-supported beam mounted with an infinite baffled subjected to a harmonic point force is considered. A concentrated mass is added to the structure to passively reduce the structural motion and sound radiation as well. Active control is performed with the use of piezoelectric actuator and PVDF sensor in conjunction with the LMS feedforward control algorithm. Hybrid control is then applied by combining the passive control element and active control mean simultaneously. The radiated sound power verse excitation frequencies is shown to evaluate the effectiveness of passive, active and hybrid control. The beam displacement distribution and radiation directivity are also shown to study the control mechanism as well as the wavenumber analysis. This work demonstrates that hybrid control can provide better acoustical control than active or passive control and also lead to providing an efficient way to the design of intelligent material structure system applied to structural sound radiation control.

2. THEORETICAL ANALYSIS

2.1 Lateral Vibration of Uniform Beam

As shown in Figure 1, a concentrated mass, M, is located at x_M. The equation of motion can then be derived as follow:

$$E_b I\frac{\partial^4 w}{\partial x^4} + [\rho_b b t_b + M\delta(x - x_M)]\frac{\partial^2 w}{\partial t^2} = p(x,t) \tag{1}$$

where w is the beam displacement; E_b the Young's modulus of the beam; I the moment of inertia; ρ_b the beam density; t_b the beam thickness; b the beam width; $p(x,t)$ the force function. Note that the damping effect is assumed small and can be neglected for simply application. The boundary conditions for a simply-supported beam are the bending moment and displacement being equal to zero at both ends.

$$M(0,t) = M(L,t) = E_b I\frac{\partial^2 w}{\partial x^2} = 0 \tag{2}$$

$$w(0,t) = w(L,t) = 0 \tag{3}$$

To solve the above equation, Fourier Analysis with the eigenfunctions of homogeneous beam vibration forming the basis for spatial expansion will be performed [11]. The beam lateral idsplacement is assumed as follow:

$$w(x,t) = e^{i\omega t}\sum_{n=1}^{\infty} W_n \sin\alpha_n x \tag{4}$$

where ω is the excitation frequency; $\alpha_n = n\pi/L_x$ is the structural wavenumber; and W_n is the n-th modal amplitude depending on the external force function. Here, the point force is applied as the disturbance input, and piezoelectric actuator is applied as the disturbance input, and piezoelectric actuator is applied as the control input; therefore, the force function can be considered as the sum of both. By substitutiong the spatial expansion of beam lateral displacement Equation (4) into Equation (1) and applying the orthogonal properties of the eigenfunctions, the equation of motion is multiplied by $\sum_{m=1}^{\infty}\sin\alpha_m x$ and integrated over the beam, then the equation of motion become

$$\sum_{n=1}^{\infty}\sum_{m=1}^{\infty}\{W_n(\alpha_n^4 - \frac{\rho_b b t_b}{E_b I}\omega^2)\frac{L}{2}\delta_{nm} - \frac{M\omega^2}{E_b I}W_n \sin\alpha_n x_M \sin\alpha_m x_M\}$$

$$= \sum_{m=1}^{\infty}\{\frac{F}{E_b I}\sin\alpha_m x_f + \frac{C_0\Lambda}{E_b I}\alpha_m(\cos\alpha_m x_1 - \cos\alpha_m x_2)\} \tag{5}$$

where F and x_f are the magnitude and location of the point force; $C_0\Lambda$ is the resultant moment induced by the piezoelectric actuator pair; C_0 is a function of material properties; Λ is the free strain of piezoelectric actuator pair subject to a voltage input; x_1 and x_2 are the coordinates of the piezoelectric actuator; and δ_{nm} is the Kronecker delta. For numerical solution purpose, the infinite series of the above equation can be approached by considering only the first few modes. In the following numerical examples, the first ten terms are

included. It is found to provide adequate convergence of beam displacement response. The above equation can then be rewritten in matrix form as follows:

$$[R]_{m\times n}\{w\}_{n\times 1} = \{p\}_{m\times 1} \tag{6}$$

where $[R]$, if $m = n$, is a symmetric modal coefficient matrix including both the beam stiffness and mass effect; $\{w\}$ is the modal amplitude vector depending on the form of force function; $\{p\}$ is the modal force vector which consists of the modal component of the point force disturbance and piezoelectric actuator. A typical element of $[R]$, $\{w\}$ and $\{P\}$ can be shown as follow:

$$R_{nm} = A_{nm} - \omega^2 B_{nm} \tag{7}$$

$$w_n = W_n \tag{8}$$

$$P_m = \frac{L}{2E_b I}(P_m^f + P_m^c) \tag{9}$$

where A_{nm}, B_{nm}, P_m^f and P_m^c are given in [10] and omitted for brevity. For free vibration analysis, Equation (6) can be reduced to the following form:

$$[A]\{W\} - \omega^2[B]\{W\} = \{O\} \tag{10}$$

One can easily solve the above generalized eigenvalue problem. Therefore, the natural frequencies of the beam with the concentrated mass can be obtained. To numerically solve Equation (6), Equation (6) can be decomposed into two independent linear system equations for both point force disturbance and piezoelectric actuator respectively as follow:

$$[R]\{w^f\} = \{p^f\}, \qquad [R]\{w^c\} = \{p^c\} \tag{11}$$

where $\{w^f\}$ and $\{w^c\}$ are the modal amplitude vactors for the point force and piezoelectric actuator which are to be determined; $\{p^f\}$ and $\{p^c\}$ are the modal force vectors for the point force and piezoelettric actuator. The modal amplitude vectos can chen be determined by solving the abover linear system equations. The beam lateral displacement due to the excitation of the point force and piezoelectric actuator can be obtained by substituting the corresponding modal amplitude vectors into Equation(4). Finally, the lateral displacement of the beam with a concentrated mass can be obtained by superposition method.

2.2 PVDF sensors' equations

For a PVDF film arranged as shown in Figure 1, the shape function can be expressed as follow:

$$\Gamma(x) = u(x - x_{s1}) - u(x - x_{s2}) \tag{12}$$

where $u(x)$ is the step function; x_{s1} and x_{s2} are the coordinates of the PVDF film. The sensor's equation can then be derived as follows [12]:

$$q(t) = \frac{t_b + t_s}{2} b_s e_{31} \int_0^L \Gamma(x) \frac{\partial^2 w}{\partial x^2} dx \tag{13}$$

where b_s is the sensor width; t_s the sensor thickness; e_{31} the piezoelectric field intensity constant. By substituting $w(x,t)$ and integrating over the beam length,

$$q(t) = e^{i\omega t}(\frac{t_b + t_s}{2} e_{31} b) \sum_{n=1}^{\infty} \alpha_n W_n (\cos \alpha_n x_{s2} - \cos \alpha_n x_{s1}) \tag{14}$$

The generated voltages can then be expressed as:

$$V(t) = \frac{q(t)}{\epsilon A} t_s \tag{15}$$

where ϵ is the permittivity of PVDF films; A is the sensor area. It is noted that the generated voltage is proportional to the slope difference detween the two edges of a PVDF film.

2.3 Sound Radiated in the Far-Field

The far-field sound pressure radiated from a vibrating surface at a point in the acoustic field, as shown in Figure 2, is given by the Rayleigh integral [13]:

$$P(\vec{r}, t) = \frac{i\omega\rho}{2\pi} \int_s \dot{w}(\vec{r}_s) \frac{e^{i\kappa R}}{R} ds \tag{16}$$

where $\vec{r}$ is the position vector of the observbation point; $\vec{r}_s$ is the position vector of the elemental surface ds; $\dot{w}(\vec{r}_s)$ is the normal velocity of ds; R is $|\vec{r} - \vec{r}_s|$; ρ is the fluid density; and $\kappa = \omega/c$ is the acoustic wavenumber. Here, the acoustic medium is air, and thus there is no feedback of the fluid motion into the structure. By substituting the beam velocity derived from Equation (4) into the Rayleigh integral, the sound pressure radiated to the far-field can be obtained [14]:

$$p(r, \theta, \phi, t) = e^{i\omega t} \sum_{n=1}^{\infty} W_n q_n \tag{17}$$

where

$$q_n = -i\omega \frac{\rho c b}{\pi} \frac{\kappa}{\alpha_n} \frac{e^{-i\kappa r}}{2r} [\frac{1 - (-1)^n e^{-i\alpha}}{1 + (\alpha/n\pi)^2}][\frac{1 - e^{-i\beta}}{\beta}] \tag{18}$$

$$\alpha = \kappa L \sin\theta \cos\phi \tag{19}$$

$$\beta = \kappa b \sin\theta \sin\phi \tag{20}$$

Under the assumption of superposition, the total radiated sound pressure can be the sum of sound pressures due to the disturbance and control inputs

$$p_t = p_f + p_c = e^{i\omega t}\sum_{n=1}^{\infty}(W_n^f + W_n^c)q_n \tag{21}$$

The total radiated sound power defined as the integral of the square of the radiated sound pressure over the hemisphere of the radiating field can then be obtained:

$$\Phi_p = \frac{1}{2\rho c}\int_s |p_t|^2 dS = \frac{r^2}{2\rho c}\int_0^{2\pi}\int_0^{\pi/2} |p_t|^2 \sin\theta d\theta d\phi \tag{22}$$

The total radiated sound power can be an index to eveluate the effectiveness of sound radiation control.

2.4 Wavenumber Analysis

The beam velocity distribution can be taken Fourier integral transrform in κ -plane.

$$\tilde{V}(\kappa_x,\ \kappa_y) = \int_{-\infty}^{\infty}\int_{-\infty}^{\infty} \dot{w}(x)e^{-i(\kappa_x x+\kappa_y y)}dxdy \tag{23}$$

where

$$\kappa_x = k\sin\theta\cos\phi \tag{24}$$

$$\kappa_y = k\sin\theta\sin\phi \tag{25}$$

therefore, the velocity transform can be expressed as:

$$\tilde{V}(\kappa_x,\ \kappa_y) = i\omega\sum_{n=1}^{\infty} W_n V_n \tag{26}$$

where

$$V_n = i\alpha_n[\frac{1-(-1)^n e^{-i\kappa_x L}}{\alpha_n^2 - \kappa_x^2}][\frac{e^{i\kappa_y b}-1}{\kappa_y}] \tag{27}$$

It is noted that the least mean square (LMS) value of the velocity transform, i.e., $|\tilde{V}|^2$, is proportional to the radiated sound power [13]. Only the wavenumber components satisfying $\kappa_x^2 + \kappa_y^2 < \kappa^2$ contribute to sound radiation into the far-field and are termed as supersonic waves. Others wavenumber components do not radiate into the far-field and are termed subsonic waves.

2.5 Cost Functions

For the use of N_s PVDF sensors, the cost function can be defined as the sum of the mean square voltages measured from the PVDF films:

$$\Psi_v = \sum_{j=1}^{N_s} |V_j|^2 \tag{28}$$

The linear quadratic optimal control theory (LQOCT) can then be applied to minimize the cost function so as to find the optimal control volages input to the piezoelectric actuators. The full analysis can be referred to [15] and omitted here for brevity. The brevity. The vibrating energy of the beam can be expressed as follow:

$$\Phi_w = \int_0^L |\ddot{w}|^2 dx \tag{31}$$

which can be used as an index to evaluate the effectiveness of vibration control.

3. NUMERICAL RESULTS AND DISCUSSIONS

A steel beam with lenght of 0.38 m, width of 0.04 m, and thickness of 2 mm is used in the simulations. The first few natural frequencies are 33.2 Hz, 128.8 Hz, 289.9 Hz, 515.4 Hz, 805.3 Hz and 1159.6 Hz. It is noted that no damping was included in the following analysis. The optimal process is suitable for controlling multiple parimary sources; however, only one harmonic point force with input parameters, $F = 0.1$ N and $x_f = 0.067$ m, was considered for the following analysis. The piezoelectric patch (G-1195) [16] and PVDF films (LDT-28 μ K) [17] are are respectively used. The piezoceramic patch is located at $x_1 = 0.285$ m, $x_2 = 0.3485$ m, and the PVDF film is located at $X_{s1} = 0.10$ m, $x_{s2} = 0.14$ m. The mass is assumed to be 50 g. In order to calculate the beam response and radiated sound pressure, it was necessary to truncate the modal sums in Equation(4). Upon cosideration of computing time and accuracy, the first 10 modes were considered, and it was found to provide sufficient convergence of series. Both the radiation directivity and beam displacement distributions were shown to demonstrate the control effectiveness of sound radiation through the beam. The radiated sound pressure is plotted in dB re 20×10^{-6} Pa over $\theta = -90°$to $90°$, while the beam displacement distribution is normalized by the largest amplitude in each case and plotted in dB along the beam length. Figure 3 shows the total radiated power verse the excitation frequencies for applying passive control only. The arrangement of the concentrated mass, PVDF sensor and piezoelectric actuator is depicted on the top of the figure. The solid line denotes the radiated power due to the disturbance alone. Several peaks right on the resonance frequencies indicate the efficient radiation for on-resonance excitation.

As the concentrated mass is added to the structure, the peaks have been shifted because the concentrated mass restructures the modal properties of the beam. For the case of M19, i.e., the mass is located at 0.19 m in the center of the beam, the even resonance modes are not affected due to the symmeric location of the mass, and the odd resonance modes are shifed to the left. A few reduction of radiated power can be observed at low frequency ranges especially for off-resonance excitation. For the case of M13, i.e., the mass near the third mode nodal point, the third resonance mode is not changed, and the other resonance peaks are shifted. Again, a few reduction of radiated power can be obsered at off-resonance frequencies for some low frequencies. Similar results can also be seen for the case of M07. Particularly, the radiated power is obviously attenuated for most off-resonance excitation below 1000Hz. With the proper selection of mass location, the resonance mode can be shifted to reduce the radiated power for on-resonance excitations of original system; however, spillover may occur at some off-resonance excitation frequencies. As the mass located away from the center of the beam, more reduction of radiated power can be achieved in the high fiequencies ranges for off-resonance excitation.

Figure 4 shows the radiated power verse the excitation frequencies for the comparison of the passive, active and hybrid control. The arrangement of the system is shown on the top of the figure. For the passive control, i. e., the mass located at 0.07m, as discussed previously the resonance peaks are shifted due to the " restructuring" effect of the mass, and a few reduction of radiated power can be obtained for off-resonance excitation. Applying active control with the use of the piezoelectric actuator and PVDF sensor, the sound radiation can be well controlled for on-resonance excitation cases; however, little attenuation can be achieved for off-resonance excitation. A new resonance peak can also be observed near 330Hz. The reform of modal properties of the stucture is due to the applied active control as discussed in[18]. As active and passive control applied simultaneously termed the hybrid control, similar results can be seen as those for active control except that hybrid control provides better sound radiation control for off-resonance cases. Therefore, with the proper selection of the active mean and passive element, hybrid control can provide better sound radiation control than either active or passive control applied individually.

Figure 5 shows the required control voltages applied to piezoelectric actuators verse excitation frequncies. The required control voltages are generally less than 25 volts sufficient for sound radiation control. As requiring high control volages, the sound radiation control can not be achieved, and spillover occur. Figure 6 shows the similar plot as that in Figure 4. It is noted that in contrast to that in Figure 4 little control can be achieved for off-resonance excitation near the fourth and fifth modes due to the improper location of the

passive element.

To further study the control mechanism of passive, active and hybrid control, figure 7 shows the beam displacement distribution, radiation directivity and the LMS of velocity transform for f=805Hz near the fifth resonance. The arrangement of the system is shown on the top of the figure. The solid line denotes the disturbance response and exhibits the fifth mode response for beam displacesent distribution as shown in Figure 7(a). As shown in Figure 7(b), the radiation directivity pattern reveals the third mode response. This can be explained by Figure 7(c). Only the wavenumber components less than the acoustic wavenumber, termed supersonic region, can radiate. As the passive element applied, the beam displacement is globally reduced so are the radiated sound pressure and the LMS of velocity transform; however, the structural vibration and sound radiation characteristics of passive control are similar to those of the original system. With applying active control, the structural response is globally reduced and reveals the fourth mode, which is a less efficient radiated mode. The corresponding radiation directivity and the LMS of velocity transform are also globally attenuated and reformed as the dipole response. For hybrid control, further radiation of beam displacement and radiated sound pressure can be achieved. Again, with the proper selection of passive element incorporated with active control mean better structural sound radiation control can be obtained.

Figure 8 shows the similar results as in Figure 7 for f=129Hz near the second resonance mode. The mass is located at the center of the beam. As applying the passive control, no control can be achieved due to the mass located right on the nodal point of the second mode. For both active and hybrid control, stuctural vibration and sound radiation can be efficiently controlled. In particular, hybrid control can provide more attenuation of sound radiation than active control. It is noted that although the residual vibrating energy are close to 111 dB for both active and hybrid control, the residual radiated power for hybrid control is 13.7 dB less than that for active control. This can also be seen from the LMS of the velocity transform as shown in Figure 8(c), because the radiated power is proportional to the sum of the supresonic wavenumber.

4. CONCLUSIONS

This work has shown the feasibility of hybrid control combining the active control mean and passive control element to attenuate structural sound radiation. A simply-supported beam mounted with an infinite rigid baffle is assumed to be subjected to a harmonically excited point force. The concentrated mass, i.e., a passive control element, is added to re-

structure the modal properties of the beam so as to achieve sound radiation control; however, the control effectiveness is limited. Active control is preformed with the use of the piezoelectric actuator and PVDF sensors to attenuate the structural sound radiation with the application of LMS feedforward control algorithm. Results show that active control can provide effective control for on-resonance excitation but not for off-resonance excitation. Hybrid control can achieve sufficient control for both on- and off-resonance excitation and provide better sound radiation control than active or passive control appied individually. Overall, hybrid control with the use of intelligent structure incorporated with passive control element can be an effective mean to attenuate structural radiated noise.

5. ACKNOWLEDGEMENTS

The author grateffully acknowledges the support of the work by National Science Council, Republic of China, under grant NSC82-0410-E-020-001.

6. REFERENCES

1. Vaicatits, R., and M. Slazak, 1980, "Noise Transmission Through Stiffened Panel," *Journal of Sound and Vibration*, 70(3), pp. 413-426.

2. Koshigoe, S., and J. W. Murdock, 1993, "A Unified Active and Passive Damping for a Plate with Piezoelectric Transducers," *Journal of Acoustical Society of America*, 93(1), pp. 346-355.

3. Stevens, J.C., and K. K. Aduja, 1991, "Recent Advances in Acive Noise Control," *AIAA Journal*, 29(7), pp. 1058-1067.

4. Bailey, T., and J. R. Hunnstf, jr., 1985, "Distributed Piezoelectric-Polymer Active Vibration Control of a Cantilever Beam, "*Journal of Gudance and Control*, 8(5), pp. 605-611.

5. Dimitriadis, E. K., C. R. Fuller, and C. A. Rogers, 1991, "Piezoelectric Actuators for Distributed Vibration Excitation of Thin Plates, "*Journal of Vibration and Acoustics*, 113, pp. 100-107.

6. Wang, B. T., and C. A. Rogers, 1991, "Modeling of Finite-Length Spatially Distributed Induced Strain Actuators for Laminate Beams and Plates,. " *Journal of Intelligent Material System and Structures*, 2(1), pp.38-58.

7. Wang, B. T., E. K. Dimitriadis, and C. R. Fuller, 1991, "Active Control of Struturally Radiated Noise Using Multiple Piezoelectric actuator," *AIAA Journal*, 29(11), pp. 1802-1809.

8. Clark, R. L., and C. R. Fuller, 1991, "Control of sound Radiation with Adaptive Structures," *Journal of Intelligent Material System and Structures*, 2(3), pp. 431-452.

9. Clark, R. L., and C. R. Fuller, 1992, "A Model Reference Approach for Implementing Active Structural Acoustic Control. " *Journal of Acoustical Society of America*, 9(3). pp. 1534-554.

10. Wang, B. T., 1992, "A Feasible Study of Hybrid Stuctural Vibration Control, " *The Proceedings of the Ninth National Conference of the Chinese Society of Mechanical Engineering*, Kaohsiung, Taiwan, pp. 449-457.

11. Sandman, B. E., 1977, "Fluid-Loaded Vibration of an Elastic Plate Carrying a Concentrated Mass, " *Journal of Acoustical Society of America* , 61(6), pp. 1503-1510.

12. Lee, C. K., and F. C. Moon, 1990, "Modal Sensors/Actuators, " *Journal of Applied Mechanics*, 57(2), pp. 434-441.

13. Fahy, F., 1985, *Sound and Structural Vibration*, Academic, Orlando, Florida.

14. Wallace, C. E., 1972, "Radiation Resistance of a Baffled Beam," *Journal of Acoustical Society of America* , 51(3), pp. 936-945.

15. Wang, B. T., 1992, "A Dynamic Simulation of Hybrid Active and Passive Control of Structural Vibration, " NSC Report, NSC81-0401-E-020-501.

16. Piezo Systems, Inc., 1990, Product Catalog.

17. Pennwalt Corporation, 1990, Piezo Film Sensor Application Notes.

18. Burdisso, R. A., and C. R. Fuller, 1992, "Theory of Feedforward Control System Eigenproperties," *Sound and Structural Vibration* , 153(3), pp. 437-452.

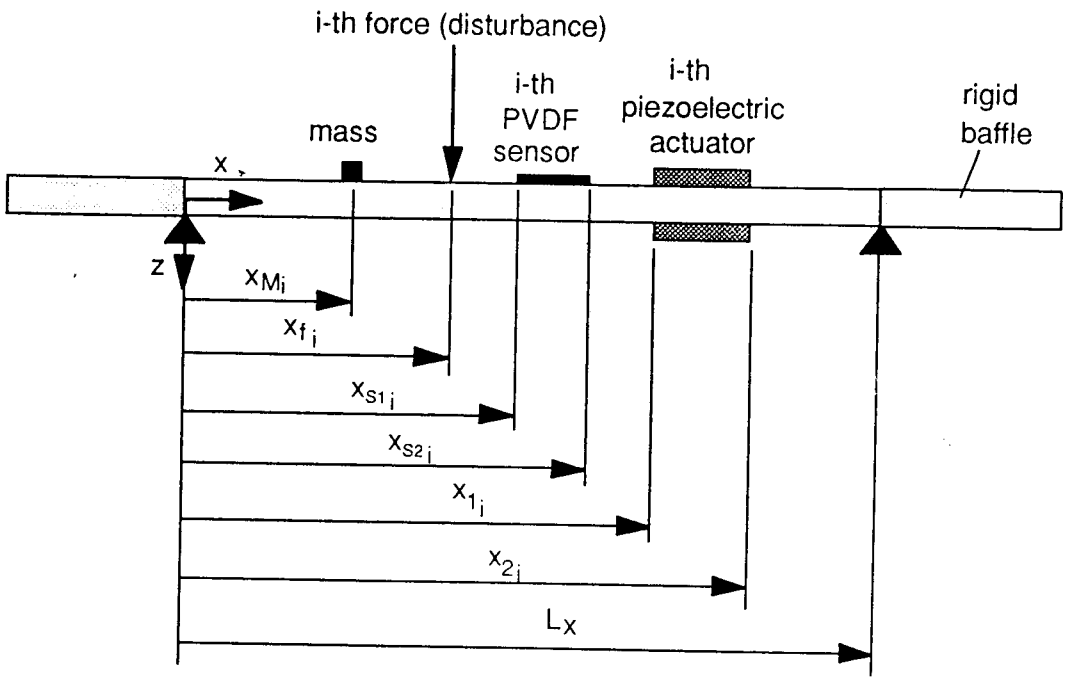

Figure 1. The arrangement and coordinates of simply-supported beam

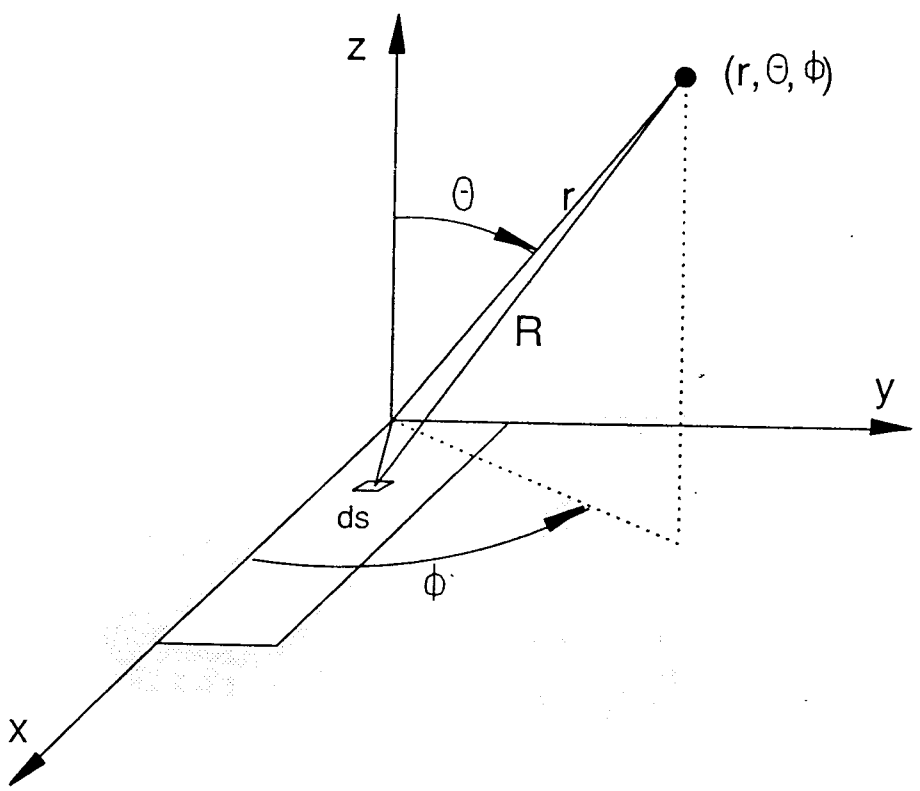

Figure 2. Sound radiated coordinates system

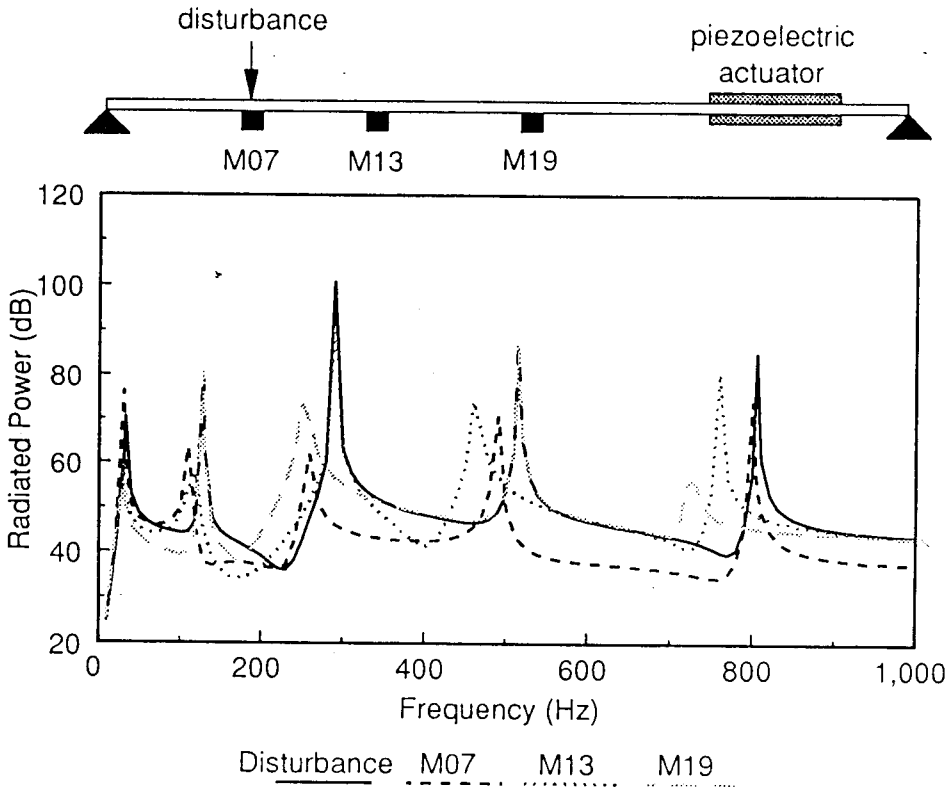

Figure 3. Radiated power verse excitation frequencies for passive control

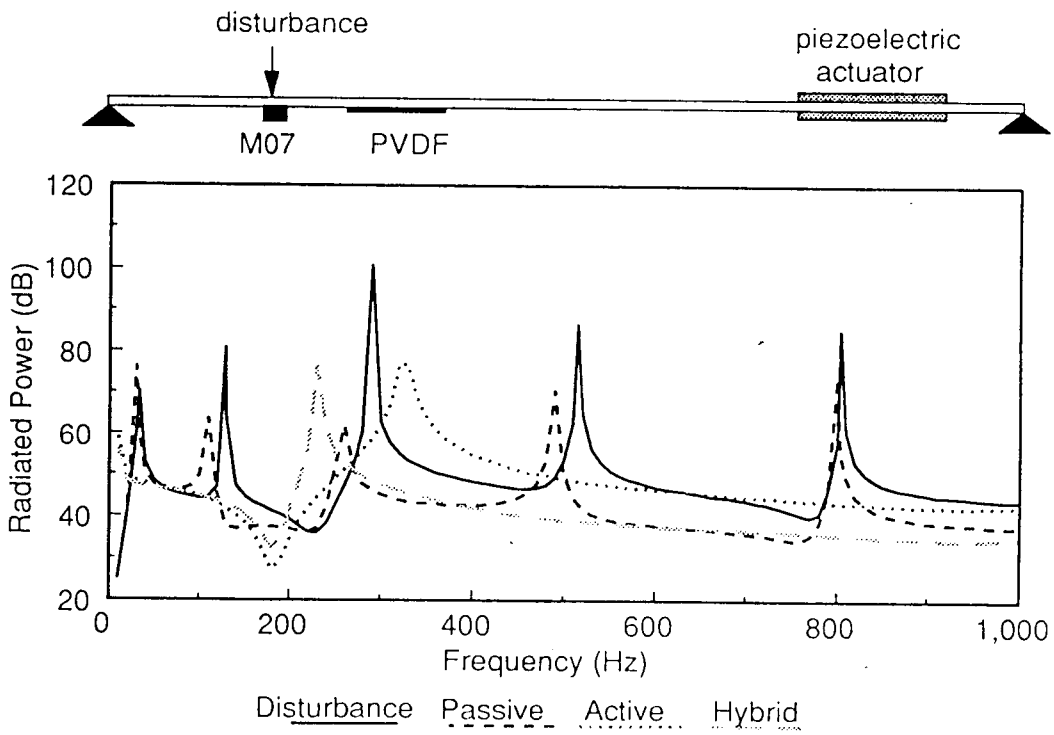

Figure 4. Radiated power verse excitation frequencies for the comparison of passive (M07), active and hybrid control

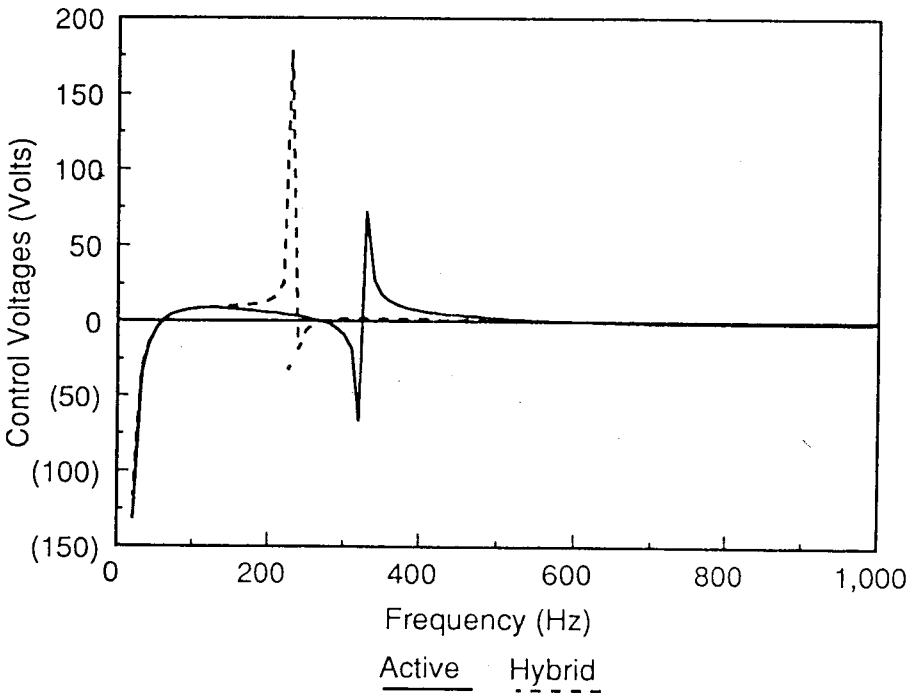

Figure 5. Control voltages verse excitation frequencies for the comparison of active and hybrid control

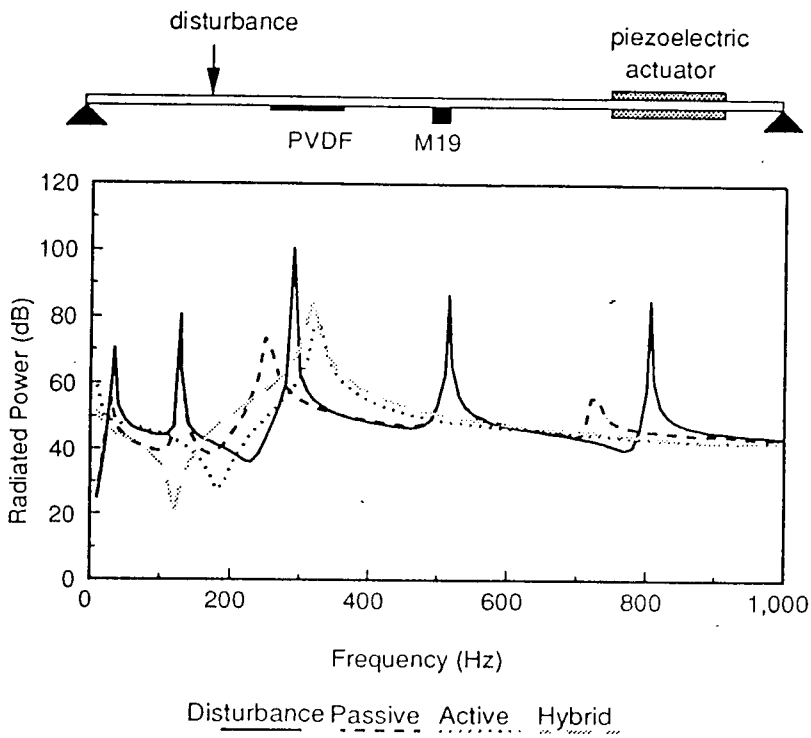

Figure 6. Radiated power verse excitation frequencies for the comparison of passive (M19), active and hybrid control

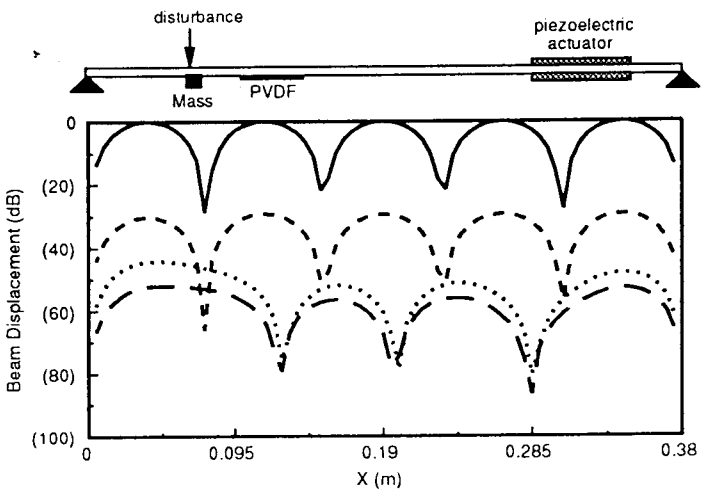

(a) beam displacement distributions

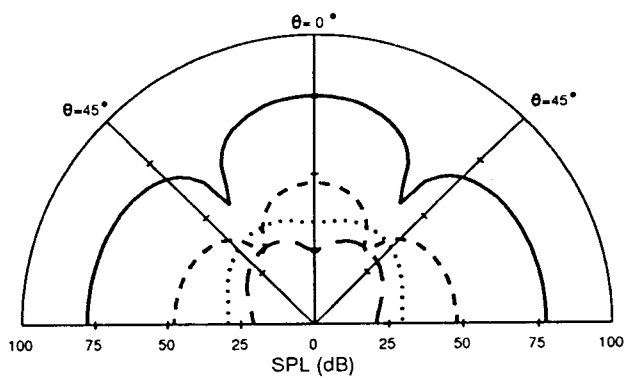

(b) radiation directivity

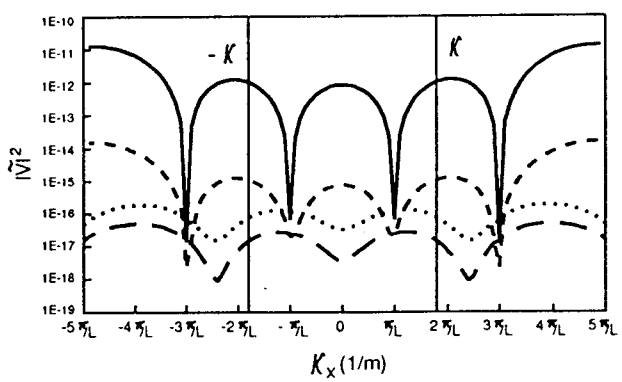

(c) LMS of velocity transform

	Disturbance	Passive	Active	Hybrid
vibrating energy (dB):	166.3	137.3	119.5	113.2
radiated power (dB):	85.4	55.2	43.2	35.5

Figure 7. A comparison of passive, active and hybrid control for f=805 Hz

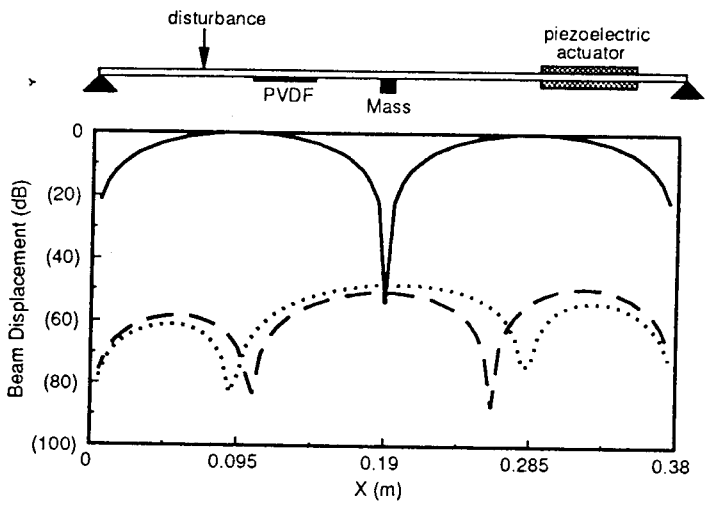

(a) beam displacement distributions

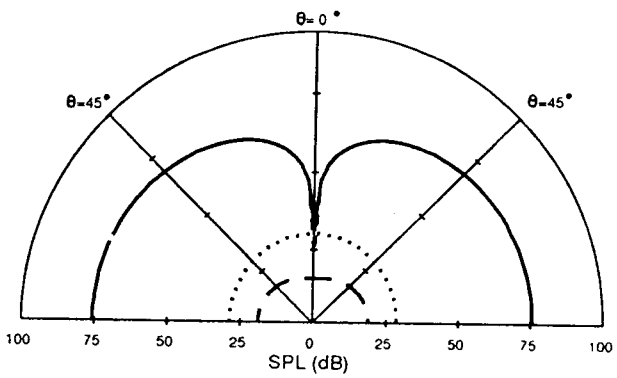

(b) radiation directivity

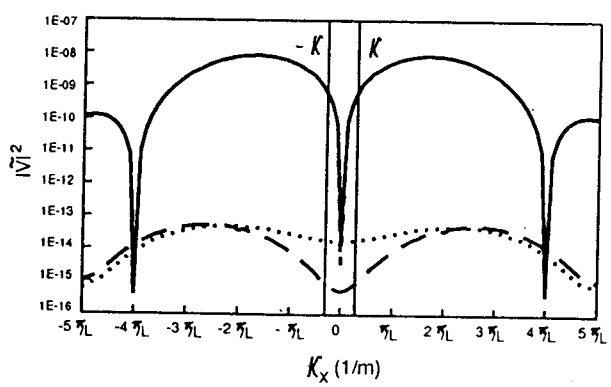

(c) LMS of velocity transform

	Disturbance	Passive	Active	Hybrid
vibrating energy (dB):	162.4	162.4	111.8	111.1
radiated power (dB):	80.9	80.9	41.8	28.1

Figure 8. A comparison of passive, active and hybrid control for f=129 Hz